

KOH activated pine tree needle leaves biochar as effective sorbent for VOCs in water

Nshirungu Theoneste^{1a}, Moon Hyun Kim^{1b}, Kurt Louis Solis^{2c}, Minoh Park^{2d} and Yongseok Hong^{2*}

¹Institute of Department of Environmental Engineering, Daegu University, 201 Daegudae-ro, Gyeongsan-si, Gyeongsangbuk-do, Republic of Korea

²Department of Environmental Systems Engineering, Korea University, 2511 Sejong-ro, Sejong City, 30019, Republic of Korea

(Received December 18, 2017, Revised March 2, 2018, Accepted March 15, 2018)

Abstract. The removal of volatile organic compounds (VOCs) from water using KOH-activated pine tree needle leaves biochar is considered a cost effective and efficient process. In this study, pine tree needle leaves were mixed with 0, 50, 100 and 200% (KOH weight/feedstock weight) of KOH, respectively. Then, the mixture was pyrolyzed at 500°C for 6 hrs. The adsorption characteristics of 10 VOCs to the biochar were tested. The results indicated that the removal efficiency of the KOH activated biochar was highest in 100% KOH-biochar. The VOC removal efficiencies of 50% and 200% KOH activated biochar were similar and the 0% KOH activated biochar showed the lowest VOC removal. The FTIR results showed that increasing the amount of KOH seemed to enhance the formation of various functional groups, such as -OH, -C=C, -O. The adsorption strength of 10 VOCs to the KOH activated biochar seemed to be increasing by the increase of the solubility of VOCs. This may suggest that the adsorption is taking place in hydrophilic sites of the biochar surface. The KOH activated pine tree needle leaves biochar can be an effective sorbent for VOCs removal in water and 100% KOH mixing seemed to provide better sorption capacity.

Keywords: pine tree needle leaves; adsorption; VOCs; activated-KOH biochar; sorbent

1. Introduction

Volatile organic compound (VOC) contamination causes various environmental concerns. Some of the more common species of pollutant VOCs are benzene, toluene, ethylbenzene, p-xylene and mesitylene, while halogenated species such as 1,2-dichloroethane, trichloroethane, chlorobenzene and 1,3-dichlorobenzene also pose a problem (Abdullah 2011, Su and Hu 2017, Nellaippan and Kumar 2018, Kah *et al.* 2017, Angin 2013, Dai *et al.* 2017, Naidu *et al.* 2016). Chronic exposure to even low concentrations of these substances in the air, surface and groundwater poses serious health risks in humans. The hazardous effect of VOC contamination was recognized as early as the 1970s (Rivett *et al.* 2011) and, since then, many countries have invested in VOC capture technology, water reclamation efforts and policy making in order to mitigate the problem (Altalyan *et al.* 2016). The target of remediation efforts is to reduce the total amount of

contaminant VOCs by half in 2020 compared to the last decade, as stated in the Gothenburg protocol (Zhang *et al.* 2017).

Conventional water treatment methods such as coagulation, flocculation, filtration, chlorination and sedimentation can be effective for volatile organic compound removal, however, adsorption is the most widely applied remediation technique for VOCs (Ahmad *et al.* 2014, Kim *et al.* 2017). During adsorption, the target molecules are trapped and collected in the pores and crevices of adsorbents (physisorption) or undergo chemical changes upon contact with the functional groups on the adsorbent surface (chemisorption). Advances in this technique involve the synthesis of new adsorbent materials with very high surface areas, high specificity for the target molecules and high porosity, as well as post-synthetic modifications in order to functionalize the existing sorbents. Researchers also consider the cost of the sorbents for practical and wide-scale applications. Materials derived from the pyrolysis of organic waste materials, otherwise known as biochar, are highly porous (Viswanathan *et al.* 2009), have economic advantages over conventional activated carbons (Ahmad *et al.* 2013) and are sustainable.

Activated biochar has been investigated in various studies (Kalinke *et al.* 2017, Agegnehu *et al.* 2017, Genovese and Lian 2017, Kah *et al.* 2017, Santos *et al.* 2016, Ahmed *et al.* 2016). Physical and chemical activation processes can be applied to carbonaceous feedstocks to enhance their physical and chemical characteristics (Naidu *et al.* 2016). The feedstocks are exposed to chemicals such as strong acids or strong bases prior to pyrolysis and gasification using steam and carbon dioxide (Naidu *et al.*

*Corresponding author, Assistant Professor

E-mail: yongseokhong@korea.ac.kr

^aMS Student

E-mail: nshirungu2013@gmail.com

^bProfessor

E-mail: moonkim@daegu.ac.kr

^cMS Student

E-mail: kurtlouisbarbasa.solis@gmail.com

^dBS Student

E-mail: atena0605@naver.com

2016). The activation process breaks some of the carbon-carbon bonds in the lignocellulose, which creates gaps and holes, thereby increasing the porosity and surface area of the biochar (Genovese and Lian 2017, Tsai *et al.* 2001). The length of the pyrolysis and activation temperature are also important factors to enhance the properties of the biochar (Naidu *et al.* 2016). Potassium hydroxide (KOH)-activated biochar has been the most widely studied and used adsorbent in the purification of air contaminated with VOCs of intermediate molecular weight (Li *et al.* 2011).

Wood and municipal wastes are the major feedstock for the preparation of biochar followed by crop residues and animal manure (Agegnehu *et al.* 2017). Plants, particularly for most tree species, regularly shed their foliage and, therefore, numerous studies have already considered the biochar feedstock potential of their dried twigs and leaves. The coniferous pine family is found in temperate regions and high altitudes in some tropical regions including South Korea. Data from the 2015 Korea Forest Service assessment of stocked forest land in South Korea shows that 2,340,000 ha (36.9%) is occupied by coniferous trees (Korea Forest Service 2015). This data translates to a vast amount of foliage for biochar feedstock, making pine tree needle leaves (PTNL) an attractive material for study.

The goal of this study is to evaluate the potential of using KOH-activated PTNL biochar for VOC removal. While some published works about PTNL biochar are available (Ahmad *et al.* 2013), present study has focused on the effect of varying the KOH loading during the activation process on the general physicochemical characteristics and overall VOC removal efficiency of the biochar. The adsorption isotherm and adsorption kinetics of 1,2-dichloroethane (DCA), benzene (BZN), trichloroethene (TCE), toluene (TOL), tetrachloroethene (PCE), chlorobenzene (CBZ), ethylbenzene (EBZ), p-xylene (PXY), 1,3,5-trimethylbenzene (TMB) and 1,3-dichlorobenzene (DCB) are investigated. The information obtained will determine the performance of KOH-activated PTNL biochar as an economically viable and effective sorbent for VOC removal.

2. Material and methods

2.1 Biochar production and characterization

Pinus tree needle leaves (PNBc) were used as a feedstock to make biochar and the biochar production procedure is summarized in Fig. 1. Approximately 50g of dried PTNL was washed by using deionized H₂O and dried for 1 day at a temperature of 80°C. The PTNL were mixed with KOH and labeled as PN0, PN50, PN100, PN200, which represent biochar without KOH, 25g of KOH in 50 g of PTNL, 50g of KOH in 50 g of PTNL and 100 g of KOH in 50 g of PTNL, respectively.

Then, the mixtures were immediately placed inside a quartz tube reactor (2.5cm diameter and 1.17m long). Both ends were sealed with Teflon adaptors and connected to 1/8 inch Teflon tubing. One end of the tubing was connected to a supply of 99.9999% N₂ with a ball flow meter and the end was connected to a fume hood to release any produced off



Fig. 1 Schematics of biochar production processes from pine tree needle leaves with KOH

gas. To remove the oxygen and moisture present in the PTNL and in the column, N₂ was flowed in at a flow rate of 100 ml/min for 2 hours at 80°C. Then, the temperature was increased to 500°C at a rate of 7.58 (±0.69) °C/min (Baronti *et al.* 2010). Once the temperature in the reactor reached the desired value, it was held at this value for 6 hours. Then, the reactor was cooled for 3 hours and the N₂ gas flow was turned off. The resulting biochar was washed with deionized water and centrifuged, 5 times, to rinse out any residual KOH. The biochar was dried in an oven for 2 days and then sieved to make it into a fine powder. The biochar yield was calculated as follows.

$$\text{Biochar Yield} = \frac{\text{Biochar(g)}}{\text{Biomass(g)}} \times 100 \quad (1)$$

The macroscopic structures and surface methodologies were visually investigated by SEM analysis (JEOL, JEOL JSM-7401F) and the surface areas were measured by BET analysis (3FLEX, Micromeritics, U.S.A.). For the FT-IR analysis, the biochar samples were finely crushed and mixed with KBr and then pelletized. Then, the IR spectra were taken in the 4000-400 cm⁻¹ range (Nicolet 380, Thermo Scientific, U.S.A.).

2.2 VOC sorption experiment

Chemical reagents of high purity, chromatography grade VOCs were purchased from Sigma-Aldrich (U.S.A.). The selected physical and chemical properties of each VOC are shown in Table 1. A 40-mL amber vial filled with 40 mL water was spiked with the VOC stock solution to make 1, 5, 10, 20, 30, 50, 75 and 100 mg/L VOC concentrations in water. Then, 0.1 g of the KOH-activated biochar was added to each vial and left to absorb for 24 hours. The equilibrated vapor concentration in the vial headspace was sampled to 100 μL and manually injected into the GC-FID for analysis.

The equilibrium sorption of VOCs into the biochar is modeled as follows:

$$C_{s,eq} = K_f C_{w,eq}^{1/n} \quad (2)$$

where K_f is the Freundlich isotherm equilibrium partitioning coefficient (L/kg) and $1/n$ is the Freundlich isotherm coefficient which describes the linearity of the isotherm curves. $C_{s,eq}$ is the quasi-steady state solid phase (biochar) VOC concentration (mg/kg) and $C_{w,eq}$ is the quasi-steady state aqueous phase VOC concentration (mg/L).

To investigate the sorption kinetics of VOCs to the biochar, 50 mg/L VOC solution with 0.1 g of biochar was prepared in 40 mL vial sealed with a Mininert valve (Supelco, Inc., U.S.A.) immediately. The vial was completely mixed using an end-over-end tumbler at 38 rpm. Gas phase VOC sample was manually taken with a volume of 100 μ L using a 250 μ L gas-tight syringe at 1, 3, 5, 10 and 24 h.

The time-dependent sorption of VOCs to the biochar was modeled as follows.

$$C_s = K_d C_{w,eq} (1 - e^{-kt}) \quad (3)$$

where C_s is a concentration of solid phase (mg/kg), $C_{s,eq}$ is a concentration of quasi-steady state solid phase (mg/kg), C_w is a concentration of aqueous phase (mg/L), $C_{w,eq}$ is a concentration of quasi-steady state aqueous phase (mg/L) and K_d is an equilibrium partitioning coefficient (L/kg).

2.3 GC-FID analysis

The main instrument used to measure the VOCs concentrations was a Shimadzu gas chromatograph with flame ionization detector (GC-FID). The column used for analysis was a 0.25 μ m Agilent DB-5 (30 m \times 0.25 mm) with a split ratio of 15.0. Ultra-pure nitrogen was used as the carrier gas with a constant flow rate of 3.0 mL/min. Both the injection and detector temperatures were 260°C. The oven was programmed at an initial temperature of 50°C for 2 min, followed by a 4°C/min increase to 85°C and then 40°C/min to 225°C and finally held at this temperature for 2 min. The auto injector device for liquid phase sampling was a Shimadzu AOC-20i, adjusted to a 2.5 μ L injection volume. The gas phase analysis of the headspace in the vial by manual injection was sampled at 100 μ L using a 250 μ L gas-tight syringe.

Table 1 Selected VOCs for this study (25°C)

| VOCs | MW (g/mol) | Log K_{ow} | Solubility in water (g/L) | Density (g/mL) | Vapor pressure | Henry's constant |
|------------------------|------------|--------------|---------------------------|----------------|----------------|------------------|
| 1,2-Dichloroethane | 98.96 | 1.48 | 8.60 | 1.25 | 10540 | 0.052 |
| Benzene | 78.1 | 2.13 | 1.53 | 0.877 | 12700 | 0.235 |
| Trichloroethene | 131.4 | 2.53 | 1.28 | 1.46 | 9900 | 0.394 |
| Toluene | 92.1 | 2.73 | 0.53 | 0.867 | 3800 | 0.260 |
| Tetrachloroethene | 165.8 | 2.88 | 0.21 | 1.62 | 2415 | 0.682 |
| Chlorobenzene | 112.6 | 2.84 | 0.48 | 1.11 | 1580 | 0.147 |
| Ethylbenzene | 106.2 | 3.15 | 0.16 | 0.863 | 1270 | 0.312 |
| p-Xylene | 106.2 | 3.12 | 0.18 | 0.857 | 1170 | 0.302 |
| 1,3,5-trimethylbenzene | 120.2 | 3.42 | 0.05 | 0.86 | 325 | 0.295 |
| 1,3-dichlorobenzene | 147.0 | 3.48 | 0.12 | 1.29 | 260 | 0.134 |

Table 2 Physical characteristics of pine tree needle leaves derived activated KOH biochar produced at 500°C

| KOH content (%) | Biochar yield (%) | Elemental Composition (%) | | | | Atomic ratio | | |
|-----------------|-------------------|---------------------------|-----------------|-----------------|------------------|--------------|------|---------|
| | | C | N | H | O | H/C | O/C | (O+N)/C |
| 0 | 34 | 75.46 (0.015) | 0.73 (0.02) | 2.23 (0.014) | 12.34 (1.005) | 0.03 | 0.16 | 0.17 |
| 50 | 38 | 45.98 (0.68) | 0.25 (0.011) | 2.37 (0.022) | 23.98 (0.262) | 0.05 | 0.52 | 0.53 |
| 100 | 40 | 28.62 (1.63) | 0.16 (0.018) | 2.02 (0.064) | 30.52 (0.586) | 0.07 | 1.07 | 1.07 |
| 200 | 44 | 17.1 (1.33) | 0.04 (0.002) | 1.41 (0.044) | 28 (0.54) | 0.08 | 1.64 | 1.64 |

3. Results and discussion

3.1 Biochar characteristics

The mass balance analysis for the biochar production at different mixing ratios with KOH are shown in Table 2. The average biochar yield was determined to be 39 (\pm 4.2)% and the decrease probably suggests that the pyrolysis removes some of functional groups and ash content (Zhang *et al.* 2015). Interestingly, the biochar yields were slightly increased by the increase of KOH content. This was considered to be the increase of functionalities and residual potassium contents in the produced biochar.

This was further supported by elemental analysis results which showed that the contents of carbon (C) was decreased from 75.5 to 17.1%, nitrogen (N) from 0.73 to 0.04% and hydrogen (H) from 2.23 to 1.42%. However, the content of oxygen (O) was increased from 12.3 to 28% by the increase of KOH contents (Azargohar and Dalai 2008).

The volatile content of the PTNL might be removed during the pyrolytic processes allowing the formation of interconnected pores, which facilitate the diffusion of KOH into the PTNL char particles, thereby resulting in a well-developed microspore structure (Mopoung *et al.* 2015, Mao *et al.* 2015). The observation was supported by SEM analysis shown in Fig. 2 (Deng and Deng 2017). In addition, the ratios of H/C, O/C and (O+N)/C were increased with increasing KOH contents, suggesting that the formation of hydrophilic surfaces and increases the site density of function groups (Mukherjee *et al.* 2011, Igalavithana *et al.* 2017).

The FTIR spectra of the PTNL biochar activated at different KOH contents are shown in Fig. 3 and the main adsorption bands are labeled. A broad peak was observed at 3340 cm^{-1} which corresponds to $-\text{OH}$ stretching. This peak is observed to increase with increasing KOH content during the activation process. Aliphatic $-\text{CH}_2$ at 2910 cm^{-1} was detected in the produced biochar.

The peaks observed at 1650 and 1400 cm^{-1} describe the $-\text{C}=\text{C}$ functional group of the aromatic compounds. The appearance of this peak in the char, particularly at pyrolysis temperatures greater than 300°C, describes the formation of double bonds from the C-H groups (Muniandy *et al.* 2014). Increasing the amount of KOH produced little to no effect in the peak intensity for the $-\text{C}=\text{C}$ functional group, suggesting that much of the C-H conversion occurs even at low KOH amounts. The peak at 1650 cm^{-1} could also be

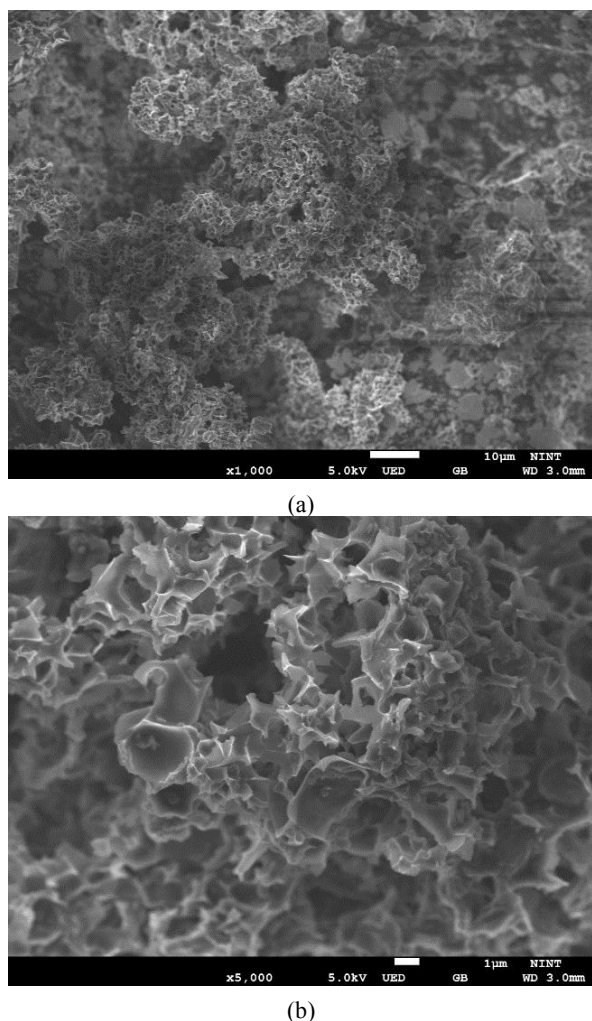


Fig. 2 SEM images of biochar PN100 at 1000x (a) and 5000x (b) magnification revealing a highly porous surface which is ideal for adsorption

due to C=O groups conjugated with aromatic rings, although this peak would be expected to decrease with increasing activation temperature and KOH content (Angin 2013), which was not observed in this experiment. The peak at 1540 cm^{-1} is assigned to the C-OH bending of alcohols and phenols. The weak peak at 1000 cm^{-1} is associated with the C-O group in the primary alcohols. There was no significant change in the intensities of these two peaks with increasing base content.

The band at 880 cm^{-1} which corresponds to the -CH out-of-plane (oop) vibration, indicated the condensation of smaller aromatic units into larger sheets (Agegnehu *et al.* 2017). This peak was also observed by Ahmad at activation temperatures of 500°C and above (Ahmad *et al.* 2013). There was a notable increase in this peak's intensity in the samples activated with KOH regardless of the KOH content. Finally, the weak peak at 670 cm^{-1} could be due to the presence of Si-H (Mopoung *et al.* 2015).

The surface area and pore characteristics of the biochar are shown in Table 3 alongside the values obtained from other studies with comparable feedstock and pyrolysis conditions. The surface area and pore volume of the biochar increased very slightly with increasing KOH loading, as

Table 3 Biochar BET Analysis

| KOH (%) | BET SA (m^2/g) | Pore Volume (cm^3/g) | | | Pore Diameter (nm) | | |
|---------|----------------------------------|--|--------|-------|--------------------|-------|-------|
| | | Meso | Micro | Total | Meso | Micro | Total |
| 0 | 3.42 | 0.01 | 0.0010 | 0.01 | 12.4 | 1.45 | 13.9 |
| 50 | 2.97 | 0.02 | 0.0009 | 0.02 | 29.2 | 1.64 | 30.8 |
| 100 | 5.66 | 0.04 | 0.0010 | 0.04 | 27.3 | 1.65 | 29.0 |
| 200 | 5.48 | 0.04 | 0.0020 | 0.04 | 28.7 | 1.62 | 30.3 |

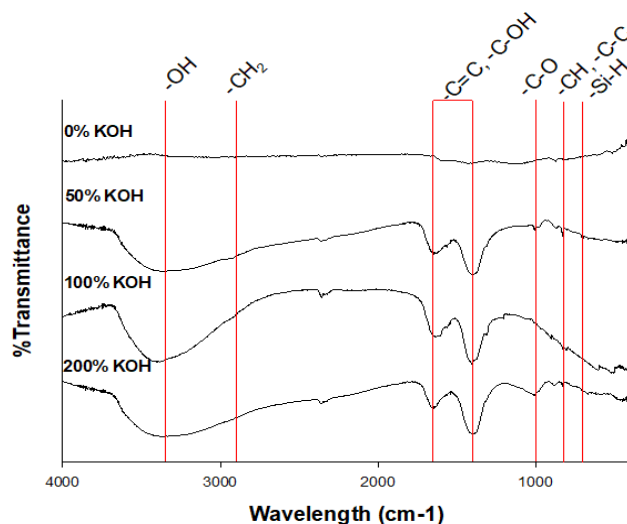


Fig. 3 FTIR spectra of PTNL biochar (BCH) with increasing KOH impregnation (0-200%) and activated at 500°C for 8 hrs

seen between a 50% KOH loading with $2.97\text{ m}^2/\text{g}$ and $0.02\text{ cm}^3/\text{g}$, respectively and 100% KOH loading with $5.66\text{ m}^2/\text{g}$ and $0.04\text{ cm}^3/\text{g}$, respectively. This shows that the KOH could have aided the decomposition of the plant material during the pyrolysis; however, this effect seemed to be minimal. These values were slightly lower than the ones reported in a previous study which also used PTNL feedstock ($13.06\text{ m}^2/\text{g}$ and $0.015\text{ cm}^3/\text{g}$) (Ahmad *et al.* 2013). The samples from 50% to 200% KOH exhibited a Type II adsorption isotherm that describes a relatively nonporous biochar. The hysteresis in the isotherm reflects the holes and cracks dotting the surface of the biochar, as observed in the SEM images. The relatively low surface area of the biochar samples is due to the tar formation that occurs when the cellulose and hemicelluloses decompose during pyrolysis at temperatures above 450°C (Lee *et al.* 2013). The tar could obstruct some pores or impede the continuity of the pores, however, this can be overcome at higher pyrolysis temperatures (Brown *et al.* 2006). Much of the pore volume of the biochar samples is mesoporous, as shown in Table 3 and by the hysteresis in the isotherms. The difference in the distribution of the cellulose, hemicellulose and lignin in different parts of the plant could be a factor affecting the observed surface area and pore characteristics of the biochar. This is demonstrated by comparing the PTNL biochar obtained in this study and the work of Ahmad *et al.* (Ahmad *et al.* 2013) with PTNL biochar (Meng *et al.* 2012), with the latter having a significantly larger surface area ($434\text{ m}^2/\text{g}$) under comparable pyrolysis conditions.

Table 4 Kinetic experiment of KOH loading from 0% up to 200% and calculations of kinetic

| Loading | Kinetics Values | Non-halogenated | | | | | Halogenated | | | | |
|---------|--|-----------------|--------|--------|--------|--------|-------------|--------|--------|--------|-------|
| | | BZN | TOL | EBZ | PXY | TMB | DCA | TCE | PCE | CBZ | DCB |
| 0% | C _{Seq} (mg g ⁻¹) | 13.8 | 13.3 | 13.6 | 15.7 | 10.3 | 9.1 | 15.4 | 15.1 | 12.9 | 12.0 |
| | k (h ⁻¹) | 0.3510 | 0.3860 | 0.4720 | 0.7790 | 0.7870 | 0.4120 | 0.5380 | 0.4790 | 0.2980 | 0.731 |
| | R ² | 0.99 | 0.98 | 0.98 | 0.98 | 0.99 | 0.99 | 0.95 | 0.94 | 0.96 | 0.98 |
| 50% | C _{Seq} (mg g ⁻¹) | 14.9 | 12.5 | 12.6 | 17.7 | 12.8 | 12.1 | 14.5 | 14.3 | 13.7 | 13.3 |
| | k (h ⁻¹) | 0.361 | 1.12 | 0.5350 | 0.952 | 1.40 | 0.3620 | 0.8340 | 0.6480 | 0.509 | 1.32 |
| | R ² | 0.99 | 0.97 | 0.97 | 0.98 | 0.96 | 0.95 | 0.95 | 0.95 | 0.98 | 0.98 |
| 100% | C _{Seq} (mg g ⁻¹) | 16.4 | 16.3 | 15.0 | 19.5 | 10.9 | 13.2 | 17.0 | 17.7 | 13.9 | 15.7 |
| | k (h ⁻¹) | 1.32 | 0.8680 | 0.940 | 1.22 | 1.45 | 0.476 | 1.21 | 0.720 | 1.14 | 1.37 |
| | R ² | 0.96 | 0.98 | 0.97 | 0.99 | 0.97 | 0.96 | 0.98 | 0.99 | 0.96 | 0.98 |
| 200% | C _{Seq} (mg g ⁻¹) | 15.3 | 13.3 | 13.6 | 15.7 | 10.3 | 9.1 | 15.4 | 15.1 | 12.9 | 12.0 |
| | k (h ⁻¹) | 0.5421 | 0.0780 | 0.7090 | 0.6910 | 0.8790 | 0.3610 | 0.8860 | 0.7440 | 0.4380 | 0.820 |
| | R ² | 0.98 | 0.97 | 0.96 | 0.98 | 0.99 | 0.95 | 0.97 | 0.95 | 0.99 | 0.98 |

3.2 Characteristics of VOCs adsorption to biochar

The kinetics of VOC adsorption by the KOH-activated biochar obtained from the PTNL was studied and the results are presented in Fig. 4. The first order adsorption kinetics parameters are summarized in Table 4. The figure shows that the adsorption equilibrium of the investigated VOCs was reached after 10 hours of exposure to the biochar. Overall, the rate of adsorption (h⁻¹) for the VOCs investigated was found out to increase with increasing KOH loading. The faster uptake could be due to the larger surface area of the biochar as well as the increased surface functional group density at a higher KOH loading. However, the VOC adsorption rate was decreased in the biochar treated with 200% KOH.

The uptake rate of 1, 2-dichloroethane was the least affected by the KOH loading. Mesitylene and 1, 3-dichlorobenzene were observed to have the fastest adsorption rates across all of the biochar, treated and untreated, used in this study. Mesitylene has three methyl groups attached to the benzene ring and, therefore, it has a higher molecular mass and lower volatility. An increase in the adsorption rate corresponding to an increase in the molecular mass of the VOCs was also observed for peat-moss biochar, however, much faster rates were reported for smaller, halogenated molecules such as TCE and PCE (Kim *et al.* 2017). While mesitylene is adsorbed faster by the biochar, more of the smaller aromatic compounds such as benzene and TCE were adsorbed at equilibrium time (10 h), as shown by their larger C_{Seq} values. The results may indicate that the larger pores or cavities were quickly occupied by bulky molecules and the smaller compounds filled in the remaining spaces. There was little difference in the uptake rate between the bulky and smaller compounds,

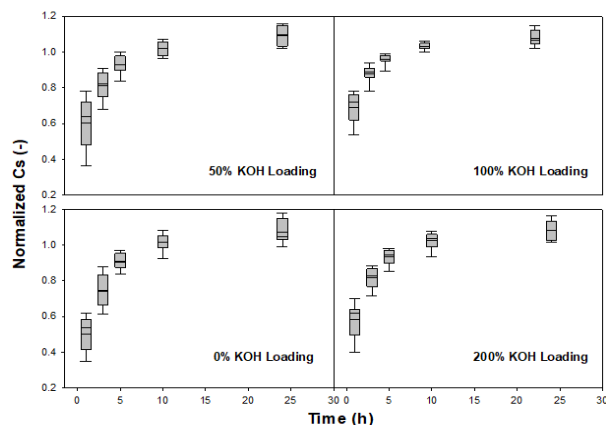


Fig. 4 The sorption kinetics of VOC on biochar at different KOH presented as normalized values

Table 5 Freundlich isotherm parameters, log K_f ((g/kg)(L/mg)^{1/n}) and 1/n, for the VOCs sorption to biochar

| Compound ID | PN0 | | | PN50 | | | PN100 | | | PN200 | | |
|-------------|--------------------|---------|----------------|--------------------|---------|----------------|--------------------|---------|----------------|--------------------|---------|----------------|
| | log K _f | 1/n | R ² | log K _f | 1/n | R ² | log K _f | 1/n | R ² | log K _f | 1/n | R ² |
| DCA | 1.72 | 0.78 | 0.99 | 1.90 | 0.87 | 0.98 | 5.74 | 0.63 | 0.92 | 2.79 | 0.82 | 0.94 |
| | (0.33) | (0.061) | | (0.52) | (0.094) | | (2.02) | (0.14) | | (1.22) | (0.16) | |
| BZN | 0.83 | 0.98 | 0.99 | 2.37 | 0.86 | 0.98 | 4.87 | 0.75 | 0.96 | 2.59 | 0.83 | 0.98 |
| | (0.24) | (0.089) | | (0.58) | (0.09) | | (1.32) | (0.11) | | (0.71) | (0.10) | |
| TCE | 1.46 | 0.74 | 0.99 | 2.32 | 0.64 | 0.94 | 3.44 | 0.82 | 0.98 | 2.35 | 0.71 | 0.99 |
| | (0.31) | (0.062) | | (1.07) | (0.14) | | (0.90) | (0.10) | | (0.41) | (0.057) | |
| TOL | 0.78 | 0.91 | 0.99 | 0.21 | 1.59 | 0.99 | 2.99 | 1.15 | 0.89 | 2.00 | 0.81 | 0.95 |
| | (0.12) | (0.043) | | (0.097) | (0.15) | | (1.84) | (0.32) | | (1.005) | (0.16) | |
| PCE | 1.59 | 0.73 | 0.99 | 1.01 | 0.92 | 0.98 | 4.08 | 0.85 | 0.97 | 0.63 | 1.23 | 0.99 |
| | (0.38) | (0.072) | | (0.38) | (0.11) | | (1.03) | (0.11) | | (0.19) | (0.10) | |
| CBZ | 0.75 | 0.97 | 0.99 | 0.64 | 1.01 | 0.99 | 3.71 | 0.93 | 0.99 | 1.91 | 0.83 | 0.99 |
| | (0.28) | (0.11) | | (0.19) | (0.089) | | (0.57) | (0.071) | | (0.28) | (0.049) | |
| EBZ | 0.88 | 0.99 | 0.99 | 1.18 | 0.84 | 0.99 | 3.88 | 0.90 | 0.99 | 1.68 | 0.82 | 0.99 |
| | (0.089) | (0.032) | | (0.18) | (0.045) | | (0.67) | (0.079) | | (0.23) | (0.044) | |
| PXY | 1.27 | 0.89 | 0.99 | 0.65 | 1.21 | 0.96 | 2.22 | 1.24 | 0.98 | 2.15 | 0.74 | 0.99 |
| | (0.30) | (0.074) | | (0.43) | (0.22) | | (0.82) | (0.18) | | (0.34) | (0.051) | |
| TMB | 1.45 | 0.85 | 0.97 | 1.64 | 0.81 | 0.99 | 5.05 | 0.76 | 0.95 | 2.31 | 0.86 | 0.96 |
| | (0.56) | (0.12) | | (0.34) | (0.066) | | (1.56) | (0.14) | | (0.89) | (0.14) | |
| DCB | 0.69 | 0.85 | 0.99 | 0.75 | 0.88 | 0.99 | 1.56 | 0.96 | 0.99 | 0.79 | 1.13 | 0.98 |
| | (0.15) | (0.059) | | (0.14) | (0.055) | | (0.36) | (0.082) | | (0.28) | (0.11) | |

or between VOCs with and without weak electron withdrawing groups such as chloride, by the treated biochar. However, it is argued that the rate limiting process in adsorption is governed by the interaction between the solute and sorbent surface through Van der Waals forces (Plazinski 2010, Danh *et al.* 2016).

The results for adsorption equilibrium experiment is shown in Fig. 5 and Freundlich isotherm parameters are summarized in Table 5. The highest absorbed VOCs in water were obtained by the biochar activated with 100% KOH for all of the compounds, while the biochar activated with 0% KOH had the lowest absorption. The sorption capacity of the KOH activated biochar was in the order of

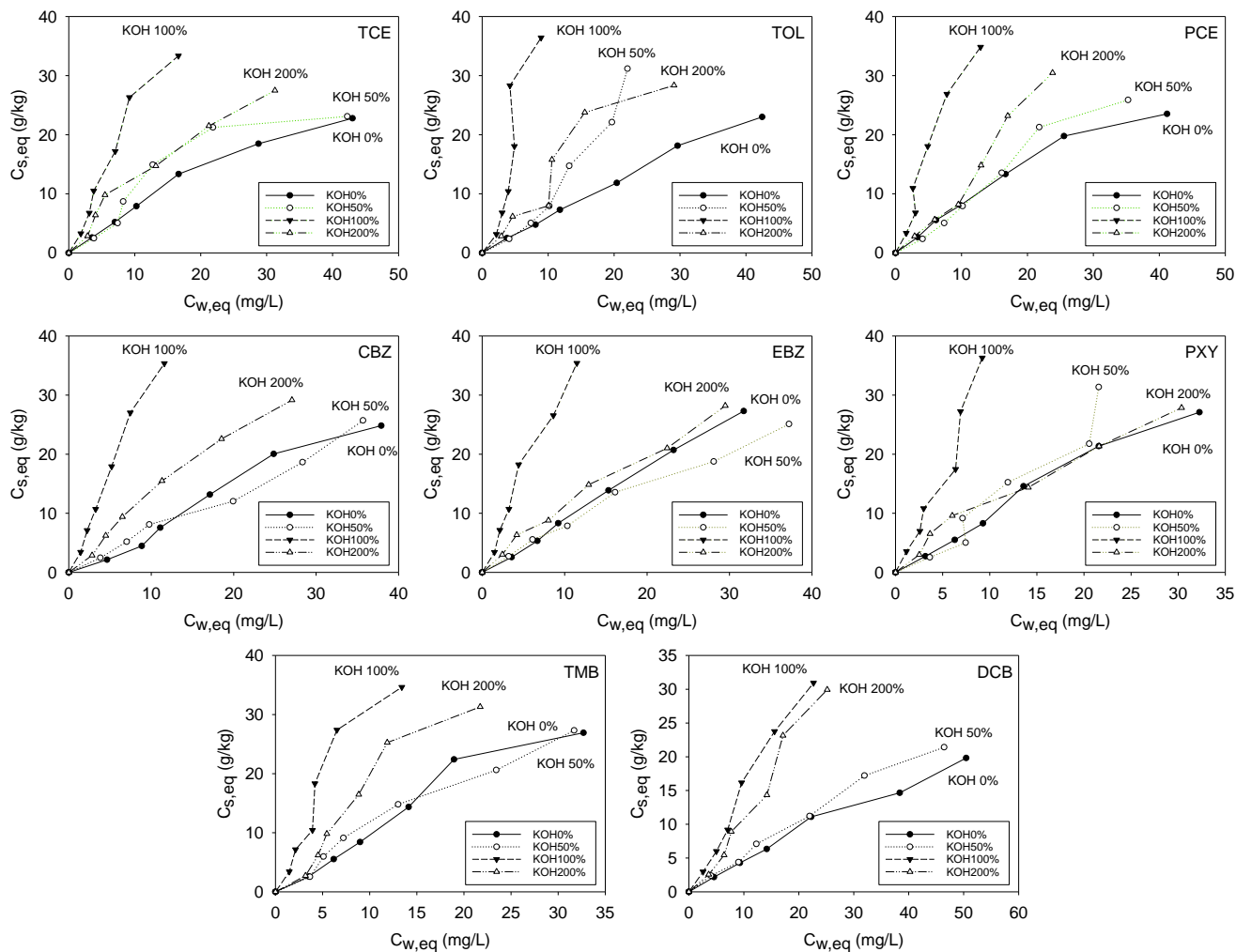


Fig. 5 The adsorption equilibrium of VOCs to the biochar produced at different KOH contents

greatest to lowest: PN100 > PN200 > PN50 > PN0. BZN, TOL, CBZ, PXY and TMB have VOC sorption capacities in the range of 35-40 g/kg, while the sorption capacities of DCA and DCB are in the range of 30-33 g/kg. For the biochar without KOH the VOC sorption capacities are varied between 10-20 g/kg. The removal efficiency of the VOCs by the activated biochar depends strongly on the interaction of the functional groups between the biochar surface and VOCs in water (Chen *et al.* 2008). The presence of KOH in the biochar derived from the PTNL increased the hydrophilic surface functionalities of the biochar, which resulted in the reduction of the freely dissolved concentration for all groups of VOCs (Oleszczuk *et al.* 2012). Hence, the sorption capacities of the biochar were increased by the increase of KOH content (%). However, if the KOH content is too high, for example 200%, then the sorption capacity was not increased and this suggests that there is an optimum KOH content for biochar activation.

In addition, the Freundlich isotherm parameter $\log K_f$ was negatively correlated with the hydrophobicity and positively correlated with the solubility. As shown in Fig. 6, the adsorption of the VOCs using the PTNL biochar pyrolyzed at 500°C shows a generally decreasing trend with $\log K_{ow}$. This trend was best observed with the PTNL

biochar activated with 100% KOH (PN100) ($R^2 = 0.62$). Considering this negative trend, it can be inferred that the more hydrophobic compound, DCB, is less adsorbed by the biochar. This can be explained by the fact that hydrophilic hydroxyl groups are present in the biochar which may cause the polar VOCs to be more adsorptive. However, this does not completely explain the decrease in the adsorption efficiency of the KOH-activated biochar which was reflected by the weak correlation of the compounds. In terms of the solubility, however, the adsorption has a positive trend in general, with the PN200 biochar having more correlation ($R^2 = 0.57$) than the other biochar types. This may be due to the presence of hydroxyl groups, which increases the affinity on adsorption of compounds that are more soluble in water.

4. Conclusion

Volatile organic compounds constitute one of the most important pollutants because of their toxicity and precursor role in photochemical smog. A number of VOC removal technologies were proposed, however some of these techniques are unsuitable for commercial application, due to

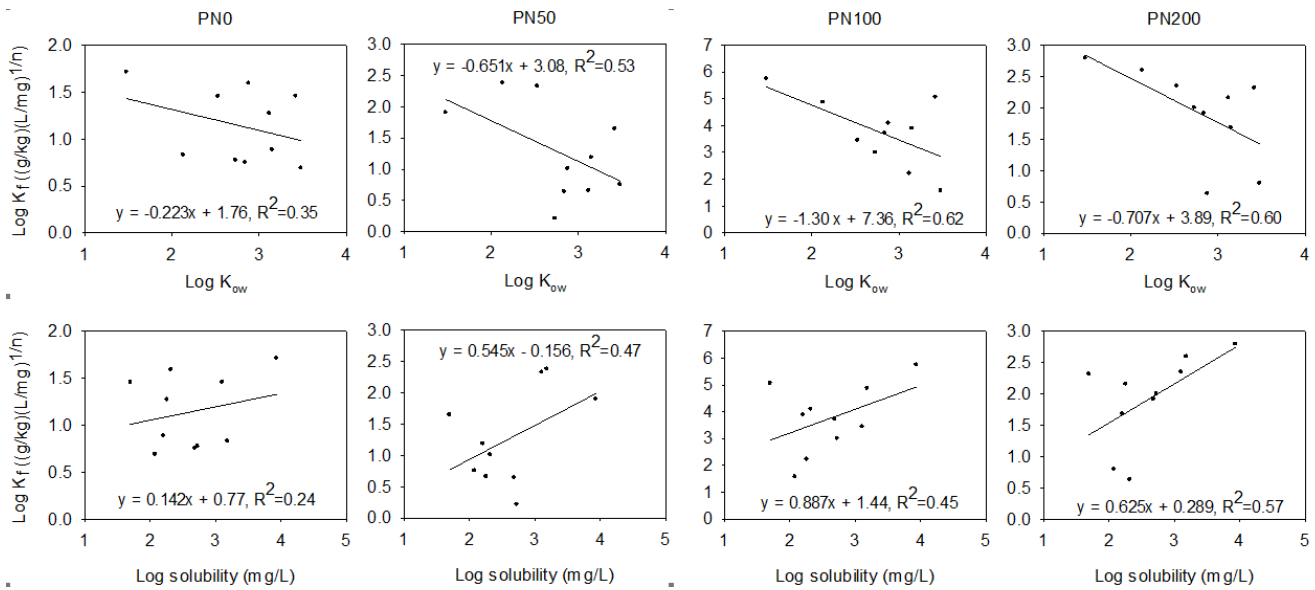


Fig. 6 Relationship between Freundlich isotherm parameter, log K_f and hydrophobicity (K_{ow}) and solubility PN0 (0% KOH), PN50 (50% KOH), PN100 (100% KOH), PN200 (200% KOH)

their low efficiency, high energy use and cost and creation of toxic byproducts. Nowadays, adsorption is the most popular VOC treatment method in practical application. As VOC adsorbents, carbonaceous materials show excellent potential, because of their large surface area, plentiful pore structure and high stability, as well as their low cost. In this study, VOC adsorption was performed by KOH activated biochar derived from PTNL. Different KOH to feedstock mass ratios, i.e., 0, 50, 100, 200%, were used to produce KOH activated biochar. The results showed that the 100% KOH biochar was the best sorbent for the removal of VOCs from water in all of the sorption experiments. The kinetics study showed that the first order kinetic constant (h^{-1}) can be applied to the experimental results and the kinetics were similar between the activated biochar. The BET surface area experiment showed that the surface area and pore volume of the biochar increased very slightly with increasing KOH loading, as seen between a 50% KOH loading with 2.97 m^2/g and 0.02 cm^3/g and 100% KOH loading with 5.66 m^2/g and 0.04 cm^3/g . This shows that KOH could have aided the decomposition of the plant material during the pyrolysis.

Acknowledgments

This research was supported by the Basic Science Research Program through the National Research Foundation of Korea (NRF) funded by the Ministry of Science, ICT and Future Planning (grant number: 2015R1C1A1A02037559) and by the Korea Ministry of Environment GAIA project (2016000550002).

References

Agegnehu, G., Srivastava, A.K. and Bird, M.I. (2017), "The role of biochar and biochar-compost in improving soil quality and crop performance: A review", *Appl. Soil Ecol.*, **119**, 156-170.

- Ahmad, M., Lee, S.S., Rajapaksha, A.U., Vinthanage, M., Cho, J.S., Lee, S.E. and Ok, Y.S. (2013), "Trichloroethylene adsorption by pine needle biochars produced at various pyrolysis temperatures", *Bioresour. Technol.*, **143**, 615-622.
- Ahmad, M., Rajapaksha, A., Lim, J., Zhang, M., Bolan, N., Mohan, D., Vithanage, M., Lee, S.S. and Ok, Y.S. (2014), "Biochar as a sorbent for contaminant management in soil and water: A review", *Chemosphere*, **99**, 19-33.
- Ahmed, M.B., Zhou, J.L., Ngo, H.H., Guo, W. and Chen, M. (2016), "Progress in the preparation and application of modified biochar for improved contaminant removal from water and wastewater", *Bioresour. Technol.*, **214**, 836-851.
- Altalyan, H.N., Jones, B.G., Bradd, J.M., Nghiem, L.D. and Alyazichi, Y.M. (2016), "Removal of volatile organic compounds (VOCs) from groundwater by reverse osmosis and nanofiltration", *J. Water Process Eng.*, **9**, 9-21.
- Angin, D. (2013), "Effect of pyrolysis temperature and heating rate on biochar obtained from pyrolysis of safflower seed press cake", *Bioresour. Technol.*, **128**, 593-597.
- Azargohar, R. and Dalai, A.K. (2008), "Steam and KOH activation of biochar: Experimental and modeling studies", *Microporous Mesoporous Mater.*, **110**(2-3), 413-421.
- Baronti, S.A., Alberti, G., Vedove, G.M., Gennaro, F.F., Fellet, G., Genesio, L., Franco, M., Peressotti, A. and Vaccari, F.P. (2010), "The biochar option to improve plant yields: First results from some field and pot experiments in Italy", *Ital. J. Agron.*, **5**(1), 3-12.
- Brown, R.A., Kercher, A.K., Nguyen, T.H., Nagle, D.C. and Ball, W.P. (2006), "Production and characterization of synthetic wood chars for use as surrogates for natural sorbents", *Org. Geochem.*, **37**(3), 321-333.
- Chen, B., Zhou, D. and Zhu, L. (2008), "Transitional adsorption and partition of nonpolar and polar aromatic contaminants by biochars of pine needles with different pyrolytic temperatures", *Environ. Sci. Technol.*, **42**(14), 5137-5143.
- Dai, H., Jing, S., Wang, H., Ma, Y., Song, W. and Kan, H. (2017), "VOC characteristics and inhalation health risks in newly renovated residences in Shanghai" *China. Sci. Total Environ.*, **577**, 73-83.
- Danh, N.T., Huy, L.N., Thi, N. and Oanh, K. (2016), "Science of the Total Environment Assessment of rice yield loss due to exposure to ozone pollution in Southern Vietnam", *Sci. Total Environ.*, **577**, 73-83.

- Environ.*, **566-567**, 1069-1079.
- Deng, J. and Deng, J. (2017), "Optically active microspheres from helical substituted polyacetylene with pendent ferrocenyl amino-acid derivative. Preparation and recycling use for direct asymmetric aldol reaction in water", *Polym.*, **125**, 200-207.
- Genovese, M. and Lian, K. (2017), "Polyoxometalate modified pine cone biochar carbon for supercapacitor electrodes", *J. Mater. Chem. A.*, **5**(8), 3939-3947.
- Igalavithana, A.D., Lee, S.E., Lee, Y.H., Tsang, D.C.W., Rinklebe, J., Kwon, E.E. and Ok, Y.S. (2017), "Heavy metal immobilization and microbial community abundance by vegetable waste and pine cone biochar of agricultural soils", *Chemosphere.*, **174**, 593-603.
- Kah, M., Sigmund, G., Xiao, F. and Hofmann, T. (2017), "Sorption of ionizable and ionic organic compounds to biochar, activated carbon and other carbonaceous materials", *Water. Res.*, **124**, 673-692.
- Kalinke, C., Oliveira, P.R., Oliveira, G.A., Mangrich, A.S., Marcolino-Junior, L.H.M. and Bergamini, M.F. (2017), "Activated biochar: Preparation, characterization and electroanalytical application in an alternative strategy of nickel determination", *Anal. Chim. Acta.*, **983**, 103-111.
- Kim, J., Lee, S.S. and Khim, J. (2017), "Peat moss-derived biochars as effective sorbents for VOCs' removal in groundwater", *Environ. Geochem. Health.*, 1-10.
- Korea Forest Service (2015), Korean Forests at a Glance; Korea Forest Service, Daejeon, Korea. english.forest.go.kr/newkfsweb/html/EngHtmlPage.do?pg=/esh/koforest/UI_KFS_0101_030000.html&mn=ENG_01_03.
- Lee, Y., Park, J., Ryu, C., Gang, K.S., Yang, W., Park, Y.K., Jung, J. and Hyun, S. (2013), "Comparison of biochar properties from biomass residues produced by slow pyrolysis at 500°C", *Bioresour. Technol.*, **148**, 196-201.
- Li, L., Liu, S. and Liu, J. (2011), "Surface modification of coconut shell based activated carbon for the improvement of hydrophobic VOC removal", *J. Hazard. Mater.*, **192**(2), 683-690.
- Naidu, M.M., Vedashree, M., Satapathy, P., Khanum, H., Ramsamy, R. and Hebbar, U. (2016), "Effect of drying methods on the quality characteristics of dill (*Anethum graveolens*) greens", *Food Chem.*, **192**, 849-856.
- Mao, H., Zhou, D., Zaher, H., Wang, S., Chen, H. and Wang, H. (2015), "Preparation of pinewood- and wheat straw-based activated carbon via a microwave-assisted potassium hydroxide treatment and an analysis of the effects of the microwave activation conditions", *BioResources.*, **10**(1), 809-821.
- Abdullah, M.D.P.A. and Chian, S.S. (2011), "Chlorinated and Nonchlorinated-Volatile Organic Compounds (VOCs) in Drinking Water of Peninsular Malaysia", *Sains Malaysiana.*, **40**(11), 1255-1261.
- Meng, H., Xia, Y. and Chen, H. (2012), "Bioremediation of surface water co-contaminated with zinc (II) and linear alkylbenzene sulfonates by *Spirulina platensis*", *Phys. Chem. Earth*, **47-48**, 152-155.
- Mopoung, S., Moonsri, P., Palas, W. and Khumpai, S. (2015), "Characterization and properties of activated carbon prepared from tamarind seeds by KOH activation for Fe (III) adsorption from aqueous solution", *Sci. World J.*, **2015**, 1-9.
- Mukherjee, A., Zimmerman, A.R. and Harris, W. (2011), "Surface chemistry variations among a series of laboratory-produced biochars", *Geoderma.*, **163**(3-4), 247-255.
- Muniandy, L., Adam, F., Mohamed, A.R. and Ng, E.P. (2014), "The synthesis and characterization of high purity mixed microporous/mesoporous activated carbon from rice husk using chemical activation with NaOH and KOH", *Microporous Mesoporous Mater.*, **197**, 316-323.
- Nellaiappan, S. and Kumar, A.S. (2018), "Selective amperometric and flow injection analysis of 1, 2-dihydroxy benzene isomer in presence of 1, 3- and 1, 4-dihydroxy benzene isomers using palladium nanoparticles-chitosan modified ITO electrode", *Sensors Actuators B Chem.*, **254**, 820-826.
- Oleszczuk, P., Hale, S.E., Lehmann, J. and Cornelissen, G. (2012), "Activated carbon and biochar amendments decrease pore-water concentrations of polycyclic aromatic hydrocarbons (PAHs) in sewage sludge", *Bioresour. Technol.*, **111**, 84-91.
- Plazinski, W. (2010), "Applicability of the film-diffusion model for description of the adsorption kinetics at the solid/solution interfaces", *Appl. Surf. Sci.*, **256**(17), 5157-5163.
- Rivett, M.O., Wealthall, G.P., Dearden, R.A. and McAlary, T.A. (2011), "Review of unsaturated-zone transport and attenuation of volatile organic compound (VOC) plumes leached from shallow source zones", *J. Contam. Hydrol.*, **123**(3-4), 130-156.
- Santos, J.M.D., Felsner, M.L., Almeida, C.A.P. and Justi, K.C. (2016), "Removal of reactive orange 107 dye from aqueous solution by activated carbon from *pinus elliottii* sawdust: A response surface methodology study", *Water, Air, Soil Pollut.*, **227**(9), 300.
- Su, S. and Hu, J. (2017), "Ultrasound assisted low-concentration VOC sensing", *Sensors Actuators B Chem.*, **254**, 1234-1241.
- Tsai, W.T., Chang, C.Y., Wang, S.Y., Chang, C., Chien, S.F. and Sun, H. (2001), "Preparation of activated carbons from corn cob catalyzed by potassium salts and subsequent gasification with CO₂", *Bioresour. Technol.*, **78**(2), 203-208.
- Viswanathan, B., Neel, P. and Varadarajan, T.K. (2009), "Methods of activation and specific applications of carbon materials", *Methods of Activation and Specific Applications of Carbon Materials*, National Centre for Catalysis Research, Chennai, India.
- Zhang, J., Liu, J. and Liu, R. (2015), "Effects of pyrolysis temperature and heating time on biochar obtained from the pyrolysis of straw and lignosulfonate", *Bioresour. Technol.*, **176**, 288-291.
- Zhang, X., Gao, B., Zheng, Y., Hu, X., Creamer, A.E. and Annable, M.D.L. (2017), "Biochar for volatile organic compound (VOC) removal: Sorption performance and governing mechanisms", *Bioresour. Technol.*, **245**, 606-614.

JK